

# AN ANALYTICAL STUDY ON URBAN INDICES AND LAND SURFACE TEMPERATURE

Subhanil GUHA<sup>✉</sup>, Himanshu GOVIL

*Department of Applied Geology, National Institute of Technology Raipur, Raipur, India*

## Highlights:

- the mean LST of the city was above 40 °C in 2013 but it is controlled in successive years by executing some eco-friendly activities;
- NDBI values are the least deviating among the three indices;
- all the indices build a moderate to strong positive correlation with LST;
- NDBI generates the best correlation followed by UI and BUI.

## Article History:

- received 13 June 2023
- accepted 15 May 2024

**Abstract.** Any urban landscape needs to investigate the rising trend of land surface temperature (LST) with its surface materials. The present study analyzes the relationship of LST with three urban indices namely normalized difference built-up index (NDBI), urban index (UI), and built-up index (BUI) (by Pearson correlation coefficient method) using nine Landsat 8 OLI and TIRS data of May from 2013 to 2021 in a tropical Indian city, Raipur. Results show that the mean LST of the city was above 40 °C in 2013 but it is controlled in successive years by executing some eco-friendly activities. All the indices build a moderate to strong positive correlation with LST. NDBI is the least deviating index and it generates the best correlation. As surface materials are directly responsible for the rise of LST, suitable ecological planning is necessary for long-term urban thermal sustainability.

**Keywords:** built-up index (BUI), Landsat, land surface temperature (LST), normalized difference built-up index (NDBI), urban index (UI).

<sup>✉</sup>Corresponding author. E-mail: [subhanilguha@gmail.com](mailto:subhanilguha@gmail.com)

## 1. Introduction

Urbanization enhances the thermal stress of a region by continuous warming process (Oke, 1988; Fu & Weng, 2016; Grimm et al., 2018). The conversion process of land accelerates the thermal status of urban areas (Chen et al., 2004; Willie et al., 2019; Zhou et al., 2019). Land surface temperature (LST) is computed by using the thermal infrared band of different satellite sensors and it is frequently used in the delineation of the heat zones of heterogeneous urban land (Oke, 1982; Weng, 2009; Tomlinson et al., 2011; Hao et al., 2016; Tran et al., 2017). The LST varies significantly by the changing ratio of the land use/land cover (LULC) categories (Fu & Weng, 2016; Guha & Govil, 2021; Cai et al., 2023; Chen et al., 2023). Various spectral indices can take an important role in extracting surface features and LST generates significant spatial, temporal, and seasonal relationships with these spectral indices (Rikimaru et al., 2002; Ogunjobi et al., 2018; Orimoloye & Ololade, 2020; Guha et al., 2022).

Built-up area extraction is an important task in urban area planning. Simultaneously, the impact of expanding

built-up areas on the rise of LST is another hot topic of discussion. Different types of built-up surface materials produce different LST values. Various band combination generates various types of built-up indices. Generally, shortwave infrared (SWIR) and near-infrared (NIR) bands are the most responsive bands for built-up extraction. Currently, the normalized difference built-up index (NDBI) is the most common and widely applied built-up index. Apart from NDBI, several built-up or urban indices have been used so far, like urban index (UI), built-up index (BUI), index-based built-up index (IBI), new built-up index (NBI), normalized built-up area index (NBAI), impervious surface area (ISA), etc. (Bonafoni, 2015).

Many recent research papers are available on LST, LULC change, climate change, and urbanization in Indian Sub-continent and surroundings (Ghaderizadeh et al., 2022; Guha et al., 2021; Jalayer et al., 2022; Tariq et al., 2021, 2022a, 2022b; Tariq & Mumtaz, 2023). Hussain et al. (2022) monitored the change in vegetation cover and its impact on the temperature in Vehari, Pakistan. Various LULC indices and their impact on LST have been discussed in Raipur, India (Guha & Govil, 2022). Arshad et al. (2022) showed that the

change in the coverage of green space (agricultural land, plantation) influence the urban heat island effect in the Lahore, Pakistan. Nichol et al. (2020) investigated urbanization and temperature indices over four decades in a multi-nucleated megacity, China's Pearl River Delta, and found that temperatures are expected to continue rising even without further urban development. Majeed et al. (2021) showed that LULC change has an association with temperature, NDBI, and NDVI in the Jhelum district of Pakistan. Tariq and Shu (2020) predicted the future rise of LST due to the fast urbanization process in Faisalabad, Pakistan. Tariq et al. (2020) established a direct correlation between LST with NDVI, NDWI, and an indirect correlation between LST with NDSI, NDBI, and built-up index in the arid Potohar region, Pakistan. Tariq et al. (2022c) compared the daytime and nighttime temperature in Islamabad, Gilgit, Peshawar, Lahore, Quetta, and Karachi station sectors of Pakistan using MODIS data.

Bonafoni (2015) attempted to compare the relationships of NDBI, UI, and BUI with LST along with some other built-up indices in Rome, Italy using six Landsat 5 TM images of dry summer months. Guha et al. (2021) investigated the seasonal variation of the LST-NDBI relationship in Raipur city, India. Zhang et al. (2009) analyzed the relationship of LST with NDBI and ISA to describe the spatial distribution and temporal variation of urban thermal patterns and associated land-use/land-cover (LULC) conditions. Chen et al. (2022) analyzed the eight-type spaces to explain that NDBI influences urban temperature more than NDVI. However, it is becoming an important task to show a relationship of LST with various built-up and urban indices for any particular season to check the sustainability

status of a tropical city. In summer season, this relationship has a special impact in any urban area. Thus, the new direction of the study is a long-term comparison of LST-NDBI, LST-UI, and LST-BUI correlation analysis on a tropical mixed urban area in the summer season by using Landsat 8 satellite data.

## 2. Materials and methods

### 2.1. Study area

The areal extent of Raipur city has been shown in Figure 1. The city is a newly developed urbanized and commercialized area. The total city extends from 21°11'22"N to 21°20'02"N and from 81°32'20"E to 81°41'50"E with an average elevation of 219 m to 322 m (Office of the Surveyor General of India, n.d.). The total area is 165 km<sup>2</sup>. Wet and dry savannah climate influences the city where summer is dry hot, winter is dry cool, and monsoon months are wet.

### 2.2. Data

Landsat 8 Operational Land Imager (OLI) and Thermal Infra-Red Sensor (TIRS) has eleven bands, in which, bands 2–5 are considered visible to near-infrared (VNIR) bands, bands 6–7 are shortwave infrared (SWIR) bands, and band 10–11 are the thermal infrared (TIR) bands. Resolutions for VNIR and SWIR bands are 30 m, while it is 100 m for the TIR band (U.S. Geological Survey, n.d.). A total of nine Landsat 8 OLI\_TIRS data of May from 2013 to 2021 were freely downloaded from Earth Explorer to conduct the whole study (Table 1).

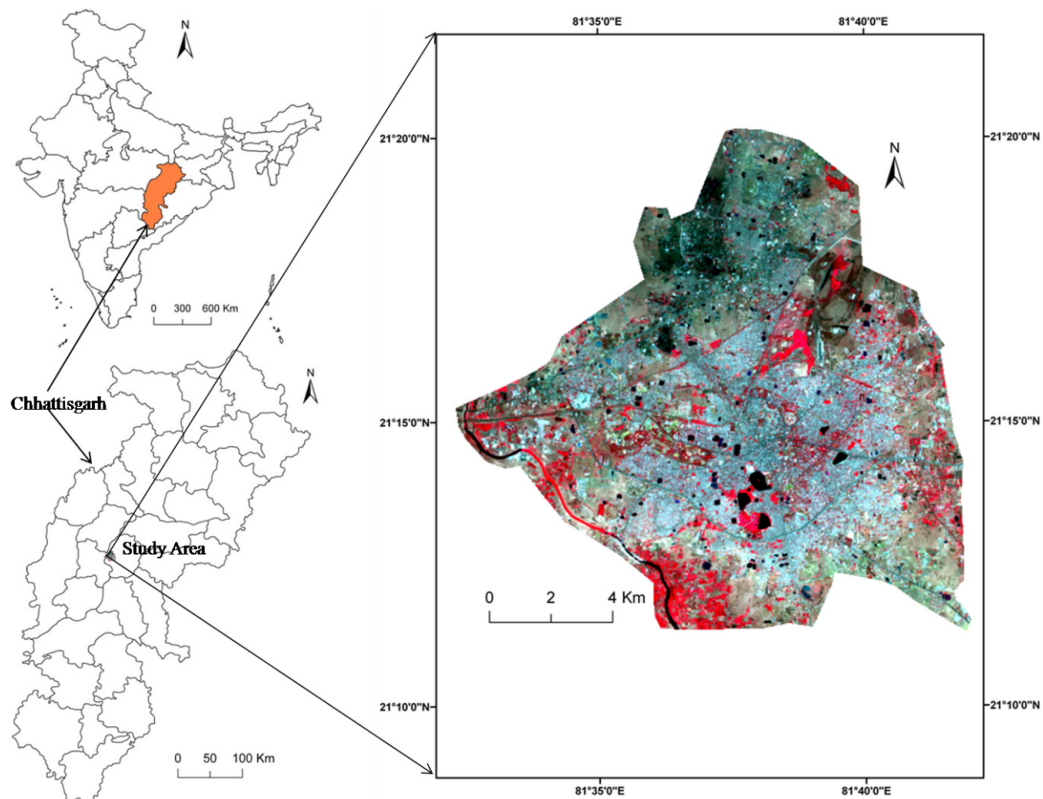


Figure 1. Location of the study area

**Table 1.** Specification of the used Landsat satellite images

Landsat scene ID	Date of acquisition	Time (UTC)*	Path/Row	Sun elevation (°)	Sun azimuth (°)	Cloud cover (%)	Earth-Sun distance (astro-nomical unit)	Reso-lution of VNIR bands (m)	Reso-lution of TIR bands (m)
LC81420452013137LGN02	2013-05-17	04:58:06	142/045	69.04	92.30	2.54	1.01	30	100
LC81420452014140LGN01	2014-05-20	04:55:38	142/045	68.56	90.40	5.46	1.01	30	100
LC81420452015127LGN01	2015-05-07	04:55:14	142/045	67.71	98.81	0.08	1.01	30	100
LC81420452016146LGN01	2016-05-25	04:55:44	142/045	68.61	87.48	0.26	1.01	30	100
LC81420452017132LGN00	2017-05-12	04:55:30	142/045	68.25	95.17	0.28	1.01	30	100
LC81420452018135LGN00	2018-05-15	04:55:08	142/045	68.27	93.32	0.30	1.01	30	100
LC81420452019138LGN00	2019-05-18	04:55:43	142/045	68.51	91.70	0.00	1.01	30	100
LC81420452020125LGN00	2020-05-04	04:55:33	142/045	67.56	100.40	3.00	1.01	30	100
LC81420452021127LGN00	2021-05-07	04:55:36	142/045	67.87	98.51	2.58	1.01	30	100

Note: \*IST = UTC + 05:30 (IST = Indian standard time, UTC = Coordinated universal time).

### 2.3. Methodology

#### 2.3.1. Computation of LST

LST is computed from Landsat TIR band (Artis & Carnahan, 1982) in which spectral radiance is determined by the following equation:

$$L_{\lambda} = \text{RadianceMultiBand} \times \text{DN} + \text{RadianceAddBand}, \quad (1)$$

where,  $L_{\lambda}$  is the spectral radiance in  $\text{Wm}^{-2}\text{sr}^{-1}\text{mm}^{-1}$ .

$$T_B = \frac{K_2}{\ln((K_1/L_{\lambda}) + 1)}, \quad (2)$$

where,  $T_B$  = brightness temperature in Kelvin (K);  $L_{\lambda}$  = spectral radiance in  $\text{Wm}^{-2}\text{sr}^{-1}\text{mm}^{-1}$ ;  $K_2$  and  $K_1$  = calibration constants;  $\varepsilon$  = surface emissivity (Sobrino et al., 2001, 2004);  $F_v$  = fractional vegetation (Carlson & Ripley, 1997):

$$F_v = \left( \frac{\text{NDVI} - \text{NDVI}_{\min}}{\text{NDVI}_{\max} - \text{NDVI}_{\min}} \right)^2, \quad (3)$$

where,  $\text{NDVI}_{\min}$  = minimum NDVI;  $\text{NDVI}_{\max}$  = maximum NDVI,  $F_v$  = fractional vegetation.

Land surface emissivity  $\varepsilon$  is calculated by the following equation:

$$\varepsilon = 0.004 \times F_v + 0.986. \quad (4)$$

Finally, LST is estimated by the following method (Weng et al., 2004):

$$\text{LST} = \frac{T_B}{1 + (\lambda \sigma T_B / (hc)) \ln \varepsilon}, \quad (5)$$

where,  $\lambda$  = effective wavelength;  $\sigma$  = Boltzmann constant ( $1.38 \times 10^{-23}$  J/K);  $h$  = Plank's constant ( $6.626 \times 10^{-34}$  Js);  $c$  = velocity of light in a vacuum ( $2.998 \times 10^8$  m/sec);  $\varepsilon$  = emissivity.

#### 2.3.2. Determination of NDBI, UI, and BUI

NDBI, UI, and BUI are applied as built-up and urban indices in the current study. NDBI is a renowned built-up index

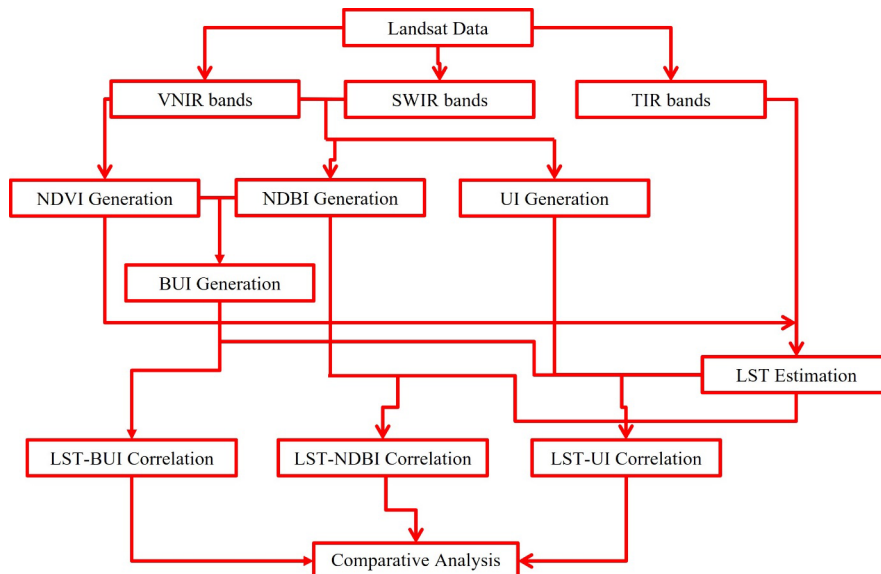


**Figure 2.** Flowchart of the methodology

that combines SWIR1 and NIR bands to capture built-up features in remote sensing studies (Zha et al., 2003). Another index is UI which combines SWIR2 and NIR bands (Kawamura et al., 1996). In both cases, the NIR band is common. The only difference is the presence of a specific SWIR band for these two indices. BUI is another built-up index used in the study (Lee et al., 2010). It is obtained by subtracting NDVI from NDBI. Hence, it combines the Red, NIR, and SWIR1 bands. These three indices are generated by the combination of NIR and SWIR bands and are considered for extracting urban characteristics. Table 2 shows the detailed description of NDBI, UI, and BUI.

**Table 2.** A detailed description of NDBI, UI, and BUI

Acronym	Description	Formulation	Reference
NDBI	Normalized difference built-up index	$(SWIR1 - NIR) / (SWIR1 + NIR)$	Zha et al. (2003)
UI	Urban index	$(SWIR2 - NIR) / (SWIR2 + NIR)$	Kawamura et al. (1996)
BUI	Built-up index	$NDBI - NDVI$	Lee et al. (2010)

A flowchart of the methodology of the study has been given in Figure 2.

### 3. Results and discussion

#### 3.1. Spatiotemporal variation in LST distribution

Figure 3 shows the spatiotemporal distribution of LST during the study period. The minimum and maximum LST ranges between 25–46 °C. In 2013, LST was significantly high. The LST drops down till 2018. Again, 2019 experiences higher LST. The city maintains the LST status in 2021 by applying some eco-friendly activities. One common feature found in the figure is that the northwest and southeast parts of the city exhibit higher LST than the remaining portions.

#### 3.2. Spatiotemporal variation in NDBI, UI, and BUI distribution

Figures 4, 5, and 6 show the spatiotemporal distribution of NDBI, UI, and BUI, respectively. The three built-up and urban indices have very little variation in their spatiotem-

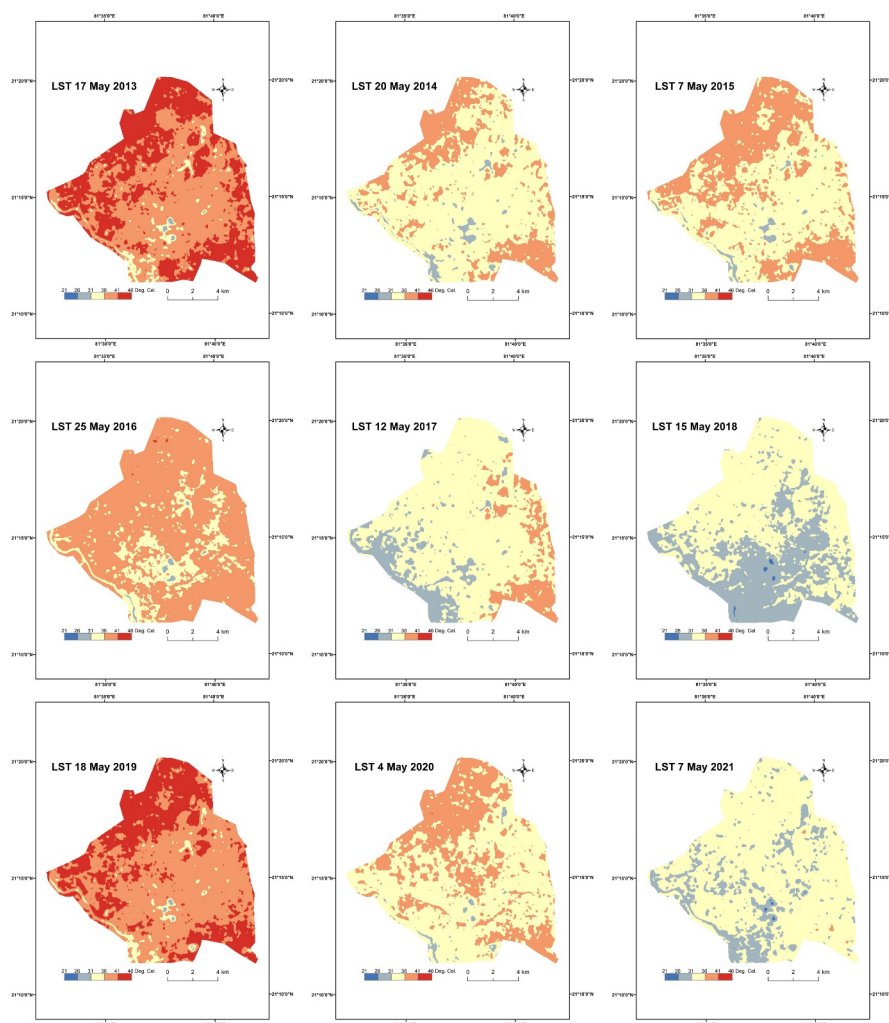


**Figure 3.** Spatiotemporal distribution of LST (2013–2021)

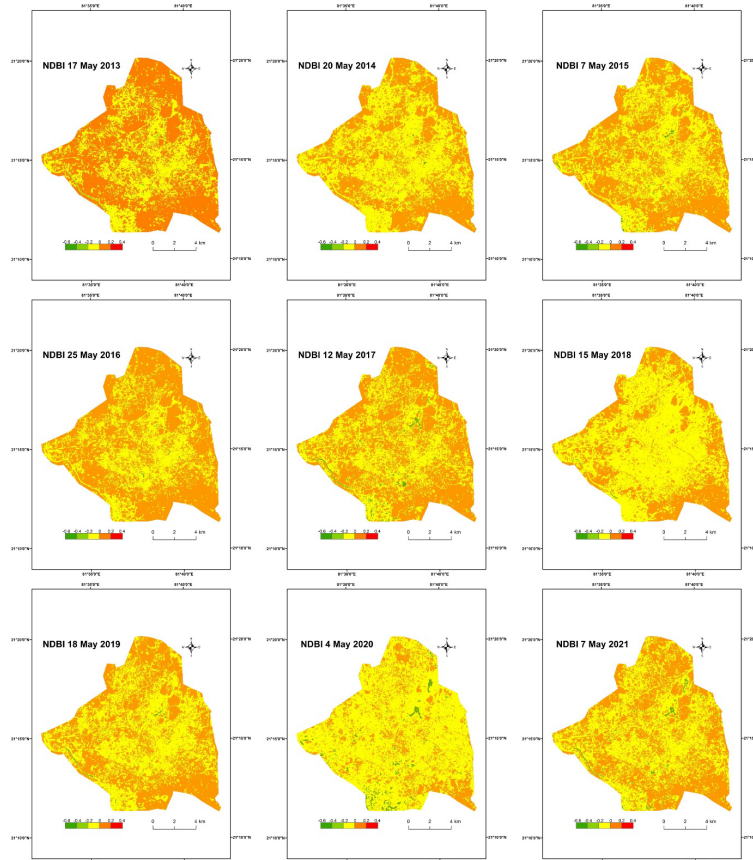


Figure 4. Spatiotemporal distribution of NDBI (2013–2021)

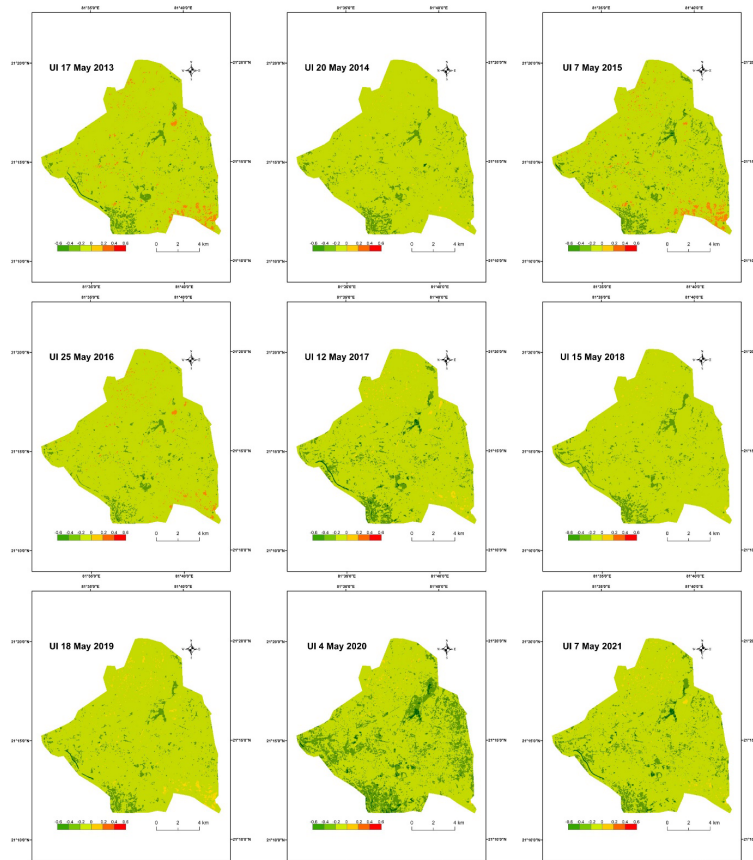
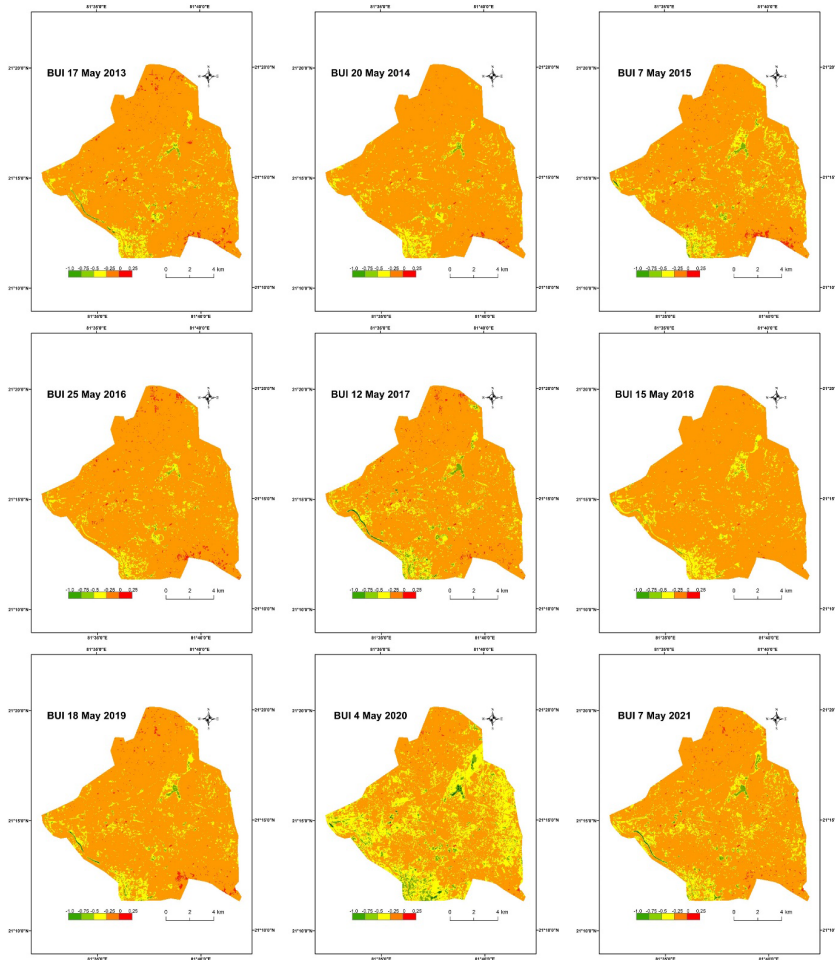


Figure 5. Spatiotemporal distribution of UI (2013–2021)



**Figure 6.** Spatiotemporal distribution of BUI (2013–2021)

poral distribution. Higher NDBI values are reflected in the periphery regions mainly the northwest and southeast corners of the city. There is no such variation in NDBI values from 2013 to 2021. The pattern is slightly different in UI distribution. The UI values are lower on the eastern and western sides. Only the northwest and southeast portions have higher UI values in some pockets. BUI has an almost similar distributional pattern. The northeast to southwest section has relatively low BUI values whereas the northwest and southeast parts have high BUI values in some small pockets. Only in 2020, the values of NDBI, UI, and BUI are considerably low. Hence, the pattern of these built-up indices is almost similar and it affects the nature of LST inside the city boundary.

Table 3 presents the statistical information on LST, NDBI, UI, and BUI. 2013 and 2019 experienced much higher LST values. 2020 and 2021 observed a significant fall in LST. NDBI values show a very stable condition throughout the period. A very low range of minimum (0.07), maximum (0.15) and mean (0.02) NDBI values have been found in nine years. The range of standard deviation values of NDBI is also very low (0.01). Actually, NDBI has the most stable values among the three indices. UI presents a slightly higher range than NDBI for the minimum (0.14), maximum

(0.28), and mean (0.08) values. The range of standard deviation is also low (0.02). The range in BUI for minimum (0.29), mean (0.12) and standard deviation (0.05) values show the highest among the three indices.

**Table 3.** Minimum, maximum, mean, and standard deviation values of LST, NDBI, UI, and BUI (2013–2021)

Date of acquisition	LST			
	Min.	Max.	Mean	Std. Dev.
17-May-13	28.75	46.00	40.28	2.22
20-May-14	26.72	39.71	34.91	1.71
07-May-15	27.01	40.65	35.53	1.80
25-May-16	28.12	41.56	37.22	1.65
12-May-17	26.39	40.63	33.33	2.16
15-May-18	25.07	36.88	31.42	1.59
18-May-19	29.48	45.54	40.21	2.11
04-May-20	28.93	41.69	35.49	1.66
07-May-21	25.30	36.79	32.06	1.45
Date of acquisition	NDBI			
	Min.	Max.	Mean	Std. Dev.
17-May-13	-0.36	0.20	0.01	0.04
20-May-14	-0.30	0.14	-0.01	0.04

End of Table 3

Date of acquisition	NDBI			
	Min.	Max.	Mean	Std. Dev.
07-May-15	-0.32	0.25	-0.01	0.05
25-May-16	-0.32	0.20	0.01	0.04
12-May-17	-0.39	0.28	-0.01	0.05
15-May-18	-0.30	0.21	-0.01	0.04
18-May-19	-0.33	0.24	-0.01	0.04
04-May-20	-0.37	0.23	-0.03	0.05
07-May-21	-0.36	0.35	-0.01	0.05
Date of acquisition	UI			
	Min.	Max.	Mean	Std. Dev.
17-May-13	-0.52	0.45	-0.07	0.06
20-May-14	-0.47	0.45	-0.10	0.05
07-May-15	-0.50	0.60	-0.09	0.06
25-May-16	-0.49	0.32	-0.08	0.05
12-May-17	-0.57	0.60	-0.10	0.07
15-May-18	-0.43	0.53	-0.10	0.05
18-May-19	-0.50	0.41	-0.08	0.06
04-May-20	-0.57	0.43	-0.15	0.08
07-May-21	-0.56	0.49	-0.11	0.07
Date of acquisition	BUI			
	Min.	Max.	Mean	Std. Dev.
17-May-13	-0.87	0.13	-0.11	0.09
20-May-14	-0.74	0.09	-0.13	0.08
07-May-15	-0.80	0.19	-0.14	0.09
25-May-16	-0.79	0.16	-0.10	0.08
12-May-17	-0.93	0.20	-0.14	0.11
15-May-18	-0.66	0.10	-0.14	0.07
18-May-19	-0.85	0.17	-0.13	0.09
04-May-20	-0.95	0.19	-0.22	0.12
07-May-21	-0.91	0.23	-0.14	0.10

Figure 7 shows the line graphs of LST and three built-up indices. Minimum, maximum, and mean values are compared for each case. The figure shows that 2013 and 2019 have two peaks in terms of LST values. NDBI is the most consistent index. UI values are quite similar to NDBI. BUI values are more variable. The minimum BUI values are nearer to -1. The overall trend of the index's values is slightly rising or neutral.

### 3.3. Variation in the relationship among LST and built-up indices

Table 4 represents the summer temporal variation of Pearson's linear correlation coefficients ( $r$ ) in LST-NDBI, LST-UI, and LST-BUI correlation analyses. All the relationships are moderately positive and stable. The strongest relationship is found between LST and NDBI (average  $r$  value is 0.64 for 9 years). UI (average  $r$  value is 0.62 for 9 years) and BUI (average  $r$  value is 0.59 for 9 years) also build a significant correlation. In 2013, 2014, and 2020, the correlation coefficient values were high above the average value for all the indices. UI builds the most consistent relationship (range is 0.15) with LST. NDBI (range is 0.18) and BUI (range is 0.18) build an equally stable relationship with LST.

Table 5 represents the temporal variation of correlation coefficients ( $r$ ) in NDBI-UI, NDBI-BUI, and UI-BUI correlation analyses. All the relationships are strongly positive and very stable. The strongest of these relationships is found between UI and BUI (average  $r$  value is 0.97). the relationship between NDBI and UI also remains very strong (average  $r$  value is 0.93). BUI and NDBI also have generated a very strong relationship (average  $r$  value is 0.88). It reflects the fact that SWIR1 and SWIR2 both bands are almost equally responsible for extracting the urban features. All three indices can be used as an influential built-up or urban index for a city area.

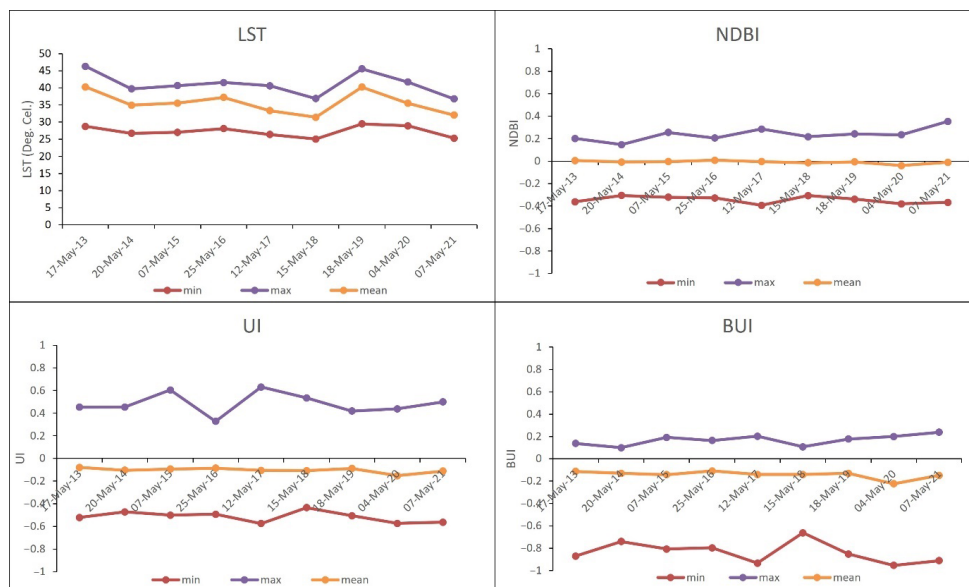


Figure 7. Line graphs showing the multivariate comparison of LST, NDBI, UI, and BUI values (2013–2021)

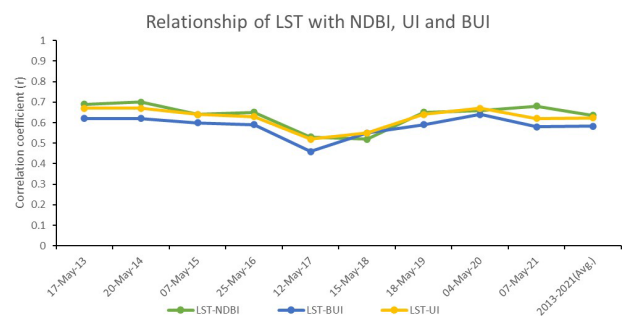
**Table 4.** Correlation coefficients ( $r$ ) of LST-NDBI, LST-UI, and LST-BUI correlation analyses from 2013–2021 (0.05 level of significance)

Date of acquisition	LST-NDBI	LST-UI	LST-BUI
17-May-13	0.69	0.67	0.62
20-May-14	0.70	0.67	0.62
07-May-15	0.64	0.64	0.60
25-May-16	0.65	0.63	0.59
12-May-17	0.53	0.52	0.46
15-May-18	0.52	0.55	0.55
18-May-19	0.65	0.64	0.59
04-May-20	0.66	0.67	0.64
07-May-21	0.68	0.62	0.58
2013–2021 (Mean)	0.64	0.62	0.59

**Table 5.** Correlation coefficients ( $r$ ) of NDBI-UI, NDBI-BUI, and UI-BUI correlation analyses from 2013–2021 (0.05 level of significance)

Date of acquisition	NDBI-UI	NDBI-BUI	UI-BUI
17-May-13	0.94	0.88	0.97
20-May-14	0.91	0.86	0.97
07-May-15	0.93	0.87	0.96
25-May-16	0.91	0.85	0.96
12-May-17	0.93	0.89	0.97
15-May-18	0.94	0.89	0.96
18-May-19	0.93	0.88	0.97
04-May-20	0.92	0.88	0.97
07-May-21	0.93	0.88	0.96
2013–2021 (Mean)	0.93	0.88	0.97

Figure 8 shows the line graphs to compare the temporal variation of LST-NDBI, LST-UI, and LST-BUI relationships. The green line shows the LST-NDBI relationship, the yellow line presents the LST-UI relationship and the blue line indicates the LST-BUI relationship. Although the three indices present a moderate to strong positive correlation, the NDBI shows the best result. This is because the SWIR1 band has a slightly better reflectance than the SWIR2 band for mixed urban materials. The correlation graph is moving significantly from 2013–2016 and again from 2019–2021. However, 2016–17 shows a falling trend and 2017–19 shows a rising trend for all the relationship graphs.

**Figure 8.** Line graphs for comparison of LST-NDBI, LST-UI, and LST-BUI relationship (2013–2021)

Some previous research papers support the outcomes of the present study. In Rome, the LST-NDBI, LST-UI, and LST-BUI, all relationships were strongly positive in the dry summer months and NDBI showed the best result followed by UI and BUI (Bonafoni, 2015). Guha et al. (2021) previously showed that the NDBI builds a moderate to a strong positive relationship ( $>0.57$ ) with LST in pre-monsoon, monsoon, post-monsoon, and winter seasons. Ezimand et al. (2021) presented that NDBI builds a better correlation with LST than fractional vegetation cover in Tartu, Estonia. According to Abir and Saha (2021), NDBI generates a moderate positive relationship with LST in the winter season. Another study reveals the fact that NDBI generates a strong relationship with LST in the Zonguldak province of Turkey (Sekertekin & Zadbagher, 2021). In the present research, LST generates a moderate to strong positive correlation (average value  $> 0.59$ ) with NDBI, UI, and BUI. Hence, the results are significantly comparable to the earlier successful research works.

## 4. Conclusions

The research estimates the values of LST, NDBI, UI, and BUI and also assesses the relationships of LST with NDBI, UI, and BUI in Raipur City using nine Landsat 8 summer images from 2013–2021. The NDBI, UI, and BUI values are almost similar over the years. Results also show that all the indices build significant moderate to strong positive relationships with LST. However, the LST-NDBI relationship (avg. value of  $r = 0.64$ ) is more positive than LST-UI (avg. value of  $r = 0.62$ ) and LST-BUI (avg. value of  $r = 0.59$ ) relationships. As the built-up area is the most important and variable land use type, the expansion and conversion of built-up land depend upon appropriate environmental planning. More green vegetation reduces the LST and more concrete building material increases the LST. Thus, the study is useful for the city planning department for future sustainable planning. In this study, only the Landsat 8 data of the summer season (May month) have been used. The results may be investigated for other seasons and other months in this particular study area. Similarly, the same procedure can be used in the other study area of different physical environment. The results can also be comparable with other satellite sensors.

## Ethics approval

This article does not contain any studies involving human participants or animals performed by any of the authors.

## Competing interests

The authors declare that they have no competing interests.

## Funding

No funding sources are available to the authors.

## Availability of data and material

The data that support the findings of this study are openly available in the earth explorer website of USGS at <https://earthexplorer.usgs.gov/>.

## References

- Abir, F. A., & Saha, R. (2021). Assessment of land surface temperature and land cover variability during winter: A spatio-temporal analysis of Pabna municipality in Bangladesh. *Environmental Challenges*, 4, Article 100167. <https://doi.org/10.1016/j.envc.2021.100167>
- Arshad, A., Zhang, W., Zaman, M. A., Dilawar, A., & Sajid, Z. (2019). Monitoring the impacts of spatio-temporal land-use changes on the regional climate of city Faisalabad, Pakistan. *Annals of GIS*, 25(1), 57–70. <https://doi.org/10.1080/19475683.2018.1543205>
- Artis, D. A., & Carnahan, W. H. (1982). Survey of emissivity variability in thermography of urban areas. *Remote Sensing of Environment*, 12(4), 313–329.
- Bonafoni, S. (2015). Spectral index utility for summer urban heating analysis. *Journal of Applied Remote Sensing*, 9(1), Article 096030. <https://doi.org/10.1117/1.JRS.9.096030>
- Cai, X., Yang, J., Zhang, Y., Xiao, X., & Xia, J. (2023). Cooling island effect in urban parks from the perspective of internal park landscape. *Humanities and Social Sciences Communications*, 10, Article 674. <https://doi.org/10.1057/s41599-023-02209-5>
- Carlson, T. N., & Ripley, D. A. (1997). On the relation between NDVI, fractional vegetation cover, and leaf area index. *Remote Sensing of Environment*, 62, 241–252. [https://doi.org/10.1016/S0034-4257\(97\)00104-1](https://doi.org/10.1016/S0034-4257(97)00104-1)
- Chen, S., Haase, D., Qureshi, S., & Firozjaei, M. K. (2022). Integrated land use and urban function impacts on land surface temperature: Implications on urban heat mitigation in Berlin with eight-type spaces. *Sustainable Cities and Society*, 83, Article 103944. <https://doi.org/10.1016/j.scs.2022.103944>
- Chen, S., Yang, J., Yu, W., Ren, J., & Xia, J. C. (2023). Relationship between urban spatial form and seasonal land surface temperature under different grid scales. *Sustainable Cities and Society*, 89, Article 104374. <https://doi.org/10.1016/j.scs.2022.104374>
- Chen, W., Liu, L., Zhang, C., Wang, J., Wang, J., & Pan, Y. (2004, September 20–24). Monitoring the seasonal bare soil areas in Beijing using multi-temporal TM images. In *Proceedings of the 2004 IEEE International Geoscience and Remote Sensing Symposium* (pp. 3379–3382), Anchorage, AK, USA.
- Ezimand, K., Azadbakht, M., & Aghighi, H. (2021). Analyzing the effects of 2D and 3D urban structures on LST changes using remotely sensed data. *Sustainable Cities and Society*, 74, Article 103216. <https://doi.org/10.1016/j.scs.2021.103216>
- Fu, P., & Weng, Q. (2016). A time series analysis of urbanization induced land use and land cover change and its impact on land surface temperature with Landsat imagery. *Remote Sensing of Environment*, 175, 205–214. <https://doi.org/10.1016/j.rse.2015.12.040>
- Ghaderizadeh, S., Abbasi-Moghadam, D., Sharifi, A., Tariq, A., & Qin, S. (2022). Multiscale Dual-Branch residual spectral-spatial network with attention for hyperspectral image classification. *IEEE Journal of Selected Topics in Applied Earth Observations and Remote Sensing*, 15, 5455–5467. <https://doi.org/10.1109/JSTARS.2022.3188732>
- Grimm, N. B., Faeth, S. H., Golubiewski, N. E., Redman, C. L., Wu, J., Bai, X., Briggs, J. M., & Grimm, N. (2008). Global change and the ecology of cities. *Science*, 319(5864), 756–760. <https://doi.org/10.1126/science.1150195>
- Guha, S., & Govil, H. (2022). Annual assessment on the relationship between land surface temperature and six remote sensing indices using Landsat data from 1988 to 2019. *Geocarto International*, 37(15), 4292–4311. <https://doi.org/10.1080/10106049.2021.1886339>
- Guha, S., & Govil, H. (2021). A long-term monthly analytical study on the relationship of LST with normalized difference spectral indices. *European Journal of Remote Sensing*, 54(1), 487–512. <https://doi.org/10.1080/22797254.2021.1965496>
- Guha, S., Govil, H., Gill, N., & Dey, A. (2021). A long-term seasonal analysis on the relationship between LST and NDBI using Landsat data. *Quaternary International*, 575–576, 249–258. <https://doi.org/10.1016/j.quaint.2020.06.041>
- Guha, S., Govil, H., Taloor, A. K., Gill, N., & Dey, A. (2022). Land surface temperature and spectral indices: A seasonal study of Raipur City. *Geodesy and Geodynamics*, 13(1), 72–82. <https://doi.org/10.1016/j.geog.2021.05.002>
- Hao, X., Li, W., & Deng, H. (2016). The oasis effect and summer temperature rise in arid regions-case study in Tarim Basin. *Scientific Reports*, 6, Article 35418. <https://doi.org/10.1038/srep35418>
- Hussain, S., Qin, S., Nasim, W., Bukhari, M. A., Mubeen, M., Fahad, S., Raza, A., Abdo, H. G., Tariq, A., Mousa, B. G., Mumtaz, F., & Aslam, M. (2022). Monitoring the dynamic changes in vegetation cover using spatio-temporal remote sensing data from 1984 to 2020. *Atmosphere*, 13(10), Article 1609. <https://doi.org/10.3390/atmos13101609>
- Jalayer, S., Sharifi, A., Abbasi-Moghadam, D., Tariq, A., & Qin, S. (2022). Modeling and predicting land use land cover spatio-temporal changes: A case study in Chalus Watershed, Iran. *IEEE Journal of Selected Topics in Applied Earth Observations and Remote Sensing*, 15, 5496–5513. <https://doi.org/10.1109/JSTARS.2022.3189528>
- Kawamura, M., Jayamana, S., & Tsujiko, Y. (1996). Relation between social and environmental conditions in Colombo Sri Lanka and the urban index estimated by satellite remote sensing data. *International Archives of Photogrammetry and Remote Sensing*, 31(B7), 321–326.
- Lee, J., Lee, S. S., & Chi, K. H. (2010). *Development of an urban classification method using a built-up index* [Conference presentation]. Sixth WSEAS International Conference on Remote Sensing, Iwate Prefectural University, Japan.
- Majeed, M., Tariq, A., Anwar, M. M., Khan, A. M., Arshad, F., Mumtaz, F., Farhan, M., Zhang, L., Zafar, A., Aziz, M., Abbasi, S., Rahman, G., Hussain, S., Waheed, M., Fatima, K., & Shaukat, S. (2021). Monitoring of land use-land cover change and potential causal factors of climate change in Jhelum District, Punjab, Pakistan, through GIS and multi-temporal satellite data. *Land*, 10(10), Article 1026. <https://doi.org/10.3390/land10101026>
- Nichol, J. E. (2005). Remote sensing of urban heat islands by day and night. *Photogrammetric Engineering & Remote Sensing*, 71, 613–621. <https://doi.org/10.14358/PERS.71.5.613>
- Office of the Surveyor General of India. (n.d.). <http://www.surveyofindia.gov.in/>
- Oke, T. R. (1988). The urban energy balance. *Progress in Physical Geography: Earth Environment*, 12(4), 471–508. <https://doi.org/10.1177/030913338801200401>
- Oke, T. R. (1982). The energetic basis of the urban heat island. *Quarterly Journal of the Royal Meteorological Society*, 108, 1–24. <https://doi.org/10.1002/qj.49710845502>
- Ogunjobi, K. O., Adamu, Y., Akinsanola, A. A., & Orimoloye, I. R. (2018). Spatio-temporal analysis of land use dynamics and its

- potential indications on land surface temperature in Sokoto Metropolis, Nigeria. *Royal Society Open Science*, 5, Article 180661. <https://doi.org/10.1098/rsos.180661>
- Orimoloye, I. R., & Ololade, O. O. (2020). Spatial evaluation of land-use dynamics in gold mining area using remote sensing and GIS technology. *International Journal of Environmental Science and Technology*, 17, 4465–4480. <https://doi.org/10.1007/s13762-020-02789-8>
- Rikimaru, A., Roy, P. S., & Miyatake, S. (2002). Tropical forest cover density mapping. *Tropical Ecology*, 43, 39–47.
- Sekertekin, A., & Zadbagher, E. (2021). Simulation of future land surface temperature distribution and evaluating surface urban heat island based on impervious surface area. *Ecological Indicators*, 122, Article 107230. <https://doi.org/10.1016/j.ecolind.2020.107230>
- Sobrino, J. A., Jiménez-Muñoz, J. C., & Paolini, L. (2004). Land surface temperature retrieval from Landsat TM5. *Remote Sensing of Environment*, 90(4), 434–440. <https://doi.org/10.1016/j.rse.2004.02.003>
- Sobrino, J. A., Raissouni, N., Li, Z. L. (2001). A comparative study of land surface emissivity retrieval from NOAA data. *Remote Sensing of Environment*, 75(2), 256–266. [https://doi.org/10.1016/S0034-4257\(00\)00171-1](https://doi.org/10.1016/S0034-4257(00)00171-1)
- Tariq, A., & Shu, H. (2020). CA-Markov Chain analysis of seasonal land surface temperature and land use land cover change using optical multi-temporal satellite data of Faisalabad, Pakistan. *Remote Sensing*, 12(20), Article 3402. <https://doi.org/10.3390/rs12203402>
- Tariq, A., & Mumtaz, F. (2023). Modeling spatio-temporal assessment of land use land cover of Lahore and its impact on land surface temperature using multi-spectral remote sensing data. *Environmental Science and Pollution Research*, 30, 23908–23924. <https://doi.org/10.1007/s11356-022-23928-3>
- Tariq, A., Yan, J., Gagnon, A. S., Khan, M. R., & Mumtaz, F. (2022a). Mapping of cropland, cropping patterns and crop types by combining optical remote sensing images with decision tree classifier and random forest. *Geo-Spatial Information Science*, 26(3), 302–320. <https://doi.org/10.1080/10095020.2022.2100287>
- Tariq, A., Yan, J., & Mumtaz, F. (2022b). Land change modeler and CA-Markov chain analysis for land use land cover change using satellite data of Peshawar, Pakistan. *Physics and Chemistry of the Earth*, 128, Article 103286. <https://doi.org/10.1016/j.pce.2022.103286>
- Tariq, A., Mumtaz, F., Zeng, X., Baloch, M. Y. J., & Moazzam, M. F. U. (2022c). Spatio-temporal variation of seasonal heat islands mapping of Pakistan during 2000–2019, using day-time and night-time land surface temperatures MODIS and meteorological stations data. *Remote Sensing Applications: Society and Environment*, 27, Article 100779. <https://doi.org/10.1016/j.rsase.2022.100779>
- Tariq, A., Riaz, I., Ahmad, Z., Yang, B., Amin, M., Kausar, R., Andleeb, S., Farooqi, M. A., & Rafiq, M. (2020). Land surface temperature relation with normalized satellite indices for the estimation of spatio-temporal trends in temperature among various land use land cover classes of an arid Potohar region using Landsat data. *Environmental of Earth Sciences*, 79, Article 40. <https://doi.org/10.1007/s12665-019-8766-2>
- Tomlinson, C. J., Chapman, L., Trones, J. E., & Baker, C. (2011). Remote sensing land surface temperature for meteorology and climatology: A review. *Meteorological Applications*, 18, 296–306. <https://doi.org/10.1002/met.287>
- Tran, D. X., Pla, F., Latorre-Carmona, P., Myint, S. W., Caetano, M., & Kieu, H. V. (2017). Characterizing the relationship between land use land cover change and land surface temperature. *ISPRS Journal of Photogrammetry and Remote Sensing*, 124, 119–132. <https://doi.org/10.1016/j.isprsjprs.2017.01.001>
- U.S. Geological Survey. (n.d.). <https://earthexplorer.usgs.gov/>
- Weng, Q. H., Lu, D. S., & Schubring, J. (2004). Estimation of land surface temperature–vegetation abundance relationship for urban heat island studies. *Remote Sensing of Environment*, 89(4), 467–483. <https://doi.org/10.1016/j.rse.2003.11.005>
- Weng, Q. (2009). Thermal infrared remote sensing for urban climate and environmental studies: Methods, applications, and trends. *ISPRS Journal of Photogrammetry and Remote Sensing*, 64(4), 335–344. <https://doi.org/10.1016/j.isprsjprs.2009.03.007>
- Willie, Y. A., Pillay, R., Zhou, L., & Orimoloye, I. R. (2019). Monitoring spatial pattern of land surface thermal characteristics and urban growth: A case study of King Williams using remote sensing and GIS. *Earth Science Informatics*, 12, 447–464. <https://doi.org/10.1007/s12145-019-00391-2>
- Zhang, R., Yang, J., & Xia, J. C. (2023). Optimal allocation of local climate zones based on heat vulnerability perspective. *Sustainable Cities and Society*, 99, Article 104981. <https://doi.org/10.1016/j.scs.2023.104981>
- Zhang, Y., Odeh, I. O. A., & Han, C. (2009). Bi-temporal characterization of land surface temperature in relation to impervious surface area, NDVI and NDBI, using a sub-pixel image analysis. *International Journal of Applied Earth Observation and Geoinformation*, 11(4), 256–264. <https://doi.org/10.1016/j.jag.2009.03.001>
- Zha, Y., Gao, J., & Ni, S. (2003). Use of normalized difference built-up index in automatically mapping urban areas from TM imagery. *International Journal of Remote Sensing*, 24, 583–594. <https://doi.org/10.1080/01431160304987>
- Zhou, D., Xiao, J., Bonafoni, S., Berger, C., Deilami, K., Zhou, Y., Frohling, S., Yao, R., Qiao, Z., & Sobrino, J. A. (2019). Satellite remote sensing of surface urban heat islands: Progress, challenges, and perspectives. *Remote Sensing*, 11(1), Article 48. <https://doi.org/10.3390/rs11010048>